Supporting Information

A carrier-less immobilization route for highly robust metal-organic hybrid enzymes

Andoni Rodríguez-Abetxuko, María Carmen Morant-Miñana, Mato Knez, Ana Beloqui

Supplemental Tables

Table S1. Protein immobilization yields calculated for @Cu, @Co, @Zn, and @Ni MOEAs fabricated in Tris, phosphate, and acetate buffer, and water.

	@Cu, %	**@Co, %**	**@Zn, %**	**@Ni, %**
Tris 30 mM, pH 7.0	100	95	100	100
Phosphate 30 mM, pH 6.0	100	70	72	51
Acetate 30 mM, pH 5.0	35	n.d.	n.d.	n.d.
Water	48	n.d.	n.d.	n.d.

n.d.: not determined

Table S2. Enzyme loading (as w%) measured for each hybrid synthesized in this study.

@Cu	**@Zn**	**@Ni**	**@Co**	**ZIF-8#1**	**ZIF-8#2**
43 %	32%	40%	30%	7.6%	4.2%

Table S3. Experimental values obtained from ICP-MS and XPS measurements for GOx@Cu-P and GOx@Cu samples.

	Cu:prot (n/n)	**N at%**	**P at%**	**Cu at%**	**C at%**	**O at%**
GOx@Cu-P	30780	8.1	6.0	4.8	51.6	29.5
GOx@Cu	400	10.3	0.0	0.2	72.0	17.5

Supplemental Figures

Figure S1. Relative concentration quantification (A) of the imidazole content within protein nanogels expressed as the ratio of the intensity given by the bands from the imidazole (υ 917 cm^{-1}) and protein (υ 1647 cm^{-1}) taken from the spectra in B. Higher Abs(υ 917)/Abs (υ 1647) ratios were attributed to nanogels with higher imidazole:protein content.
Protein:VIm molar ratios of 1:2000 and 1:3000 were discarded for this study as they led to the formation of insoluble aggregates in the synthesis procedure.

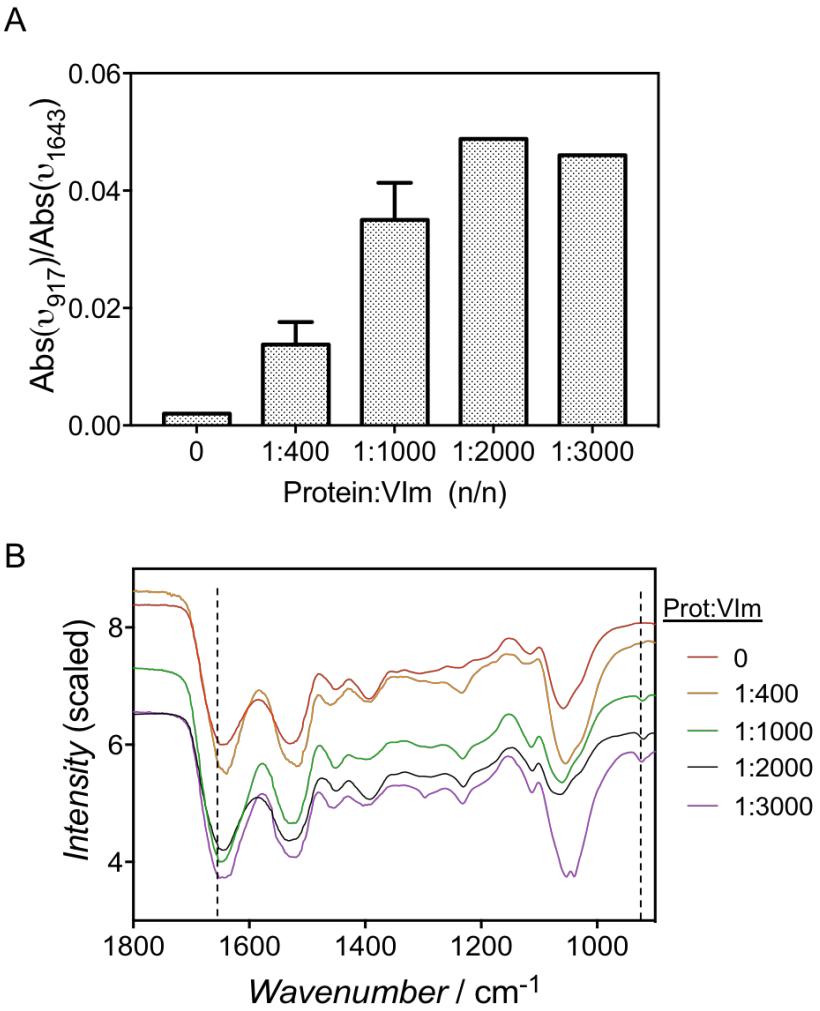

Figure S2. Measurement of the averaged size of free GOx and GOx@imNG nanogels by DLS (A) and AFM (B). Z-profile was extracted from AFM image for size measurement.

A

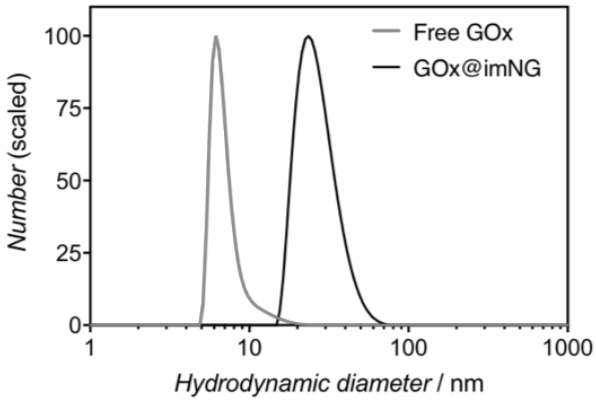

B

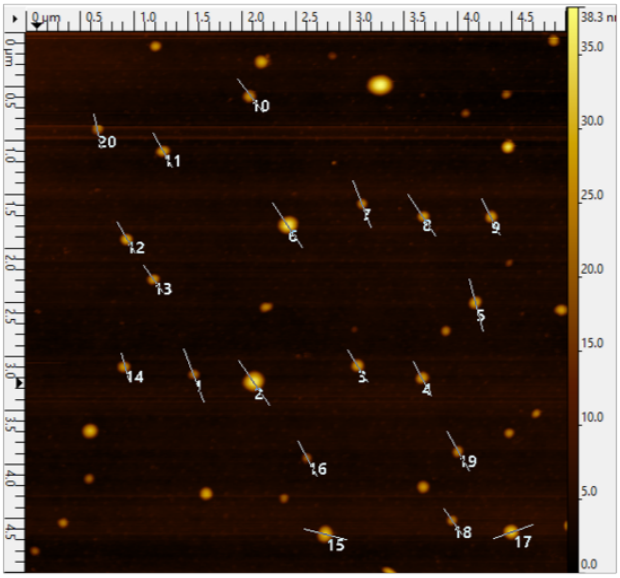

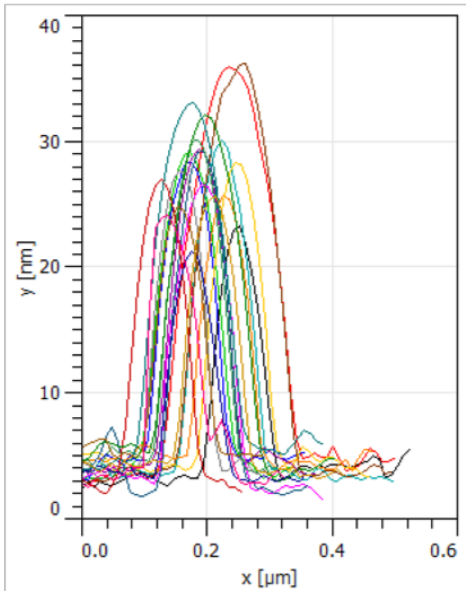

Figure S3. Normalized circular dichroism spectra of free GOx and GOx-polymer nanoconjugate (GOx@imNG).

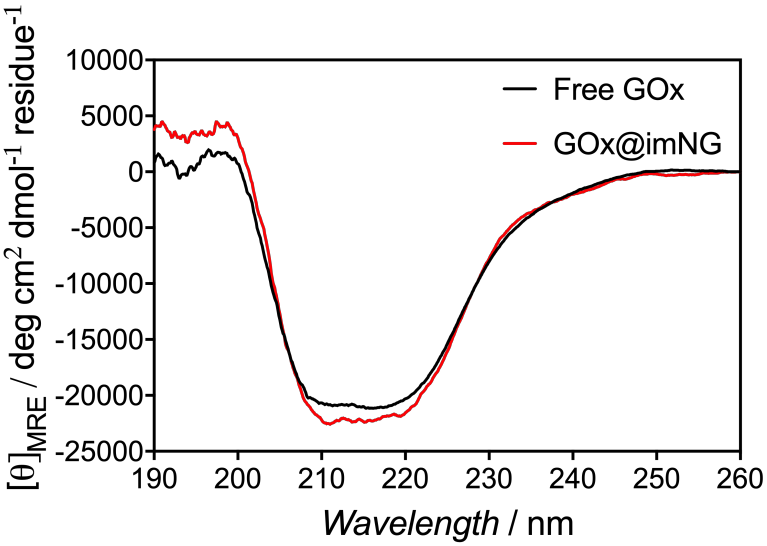

Figure S4. EDX spectra of @Cu, @Zn, @Ni, and @Co MOEAs. Metal cations are clearly observed in EDX spectra of respective MOEAs together with C, O, N signals from the protein-polymer nanoconjugates and Si signal coming from the substrate in which the MOEAs were deposited for the measurement.

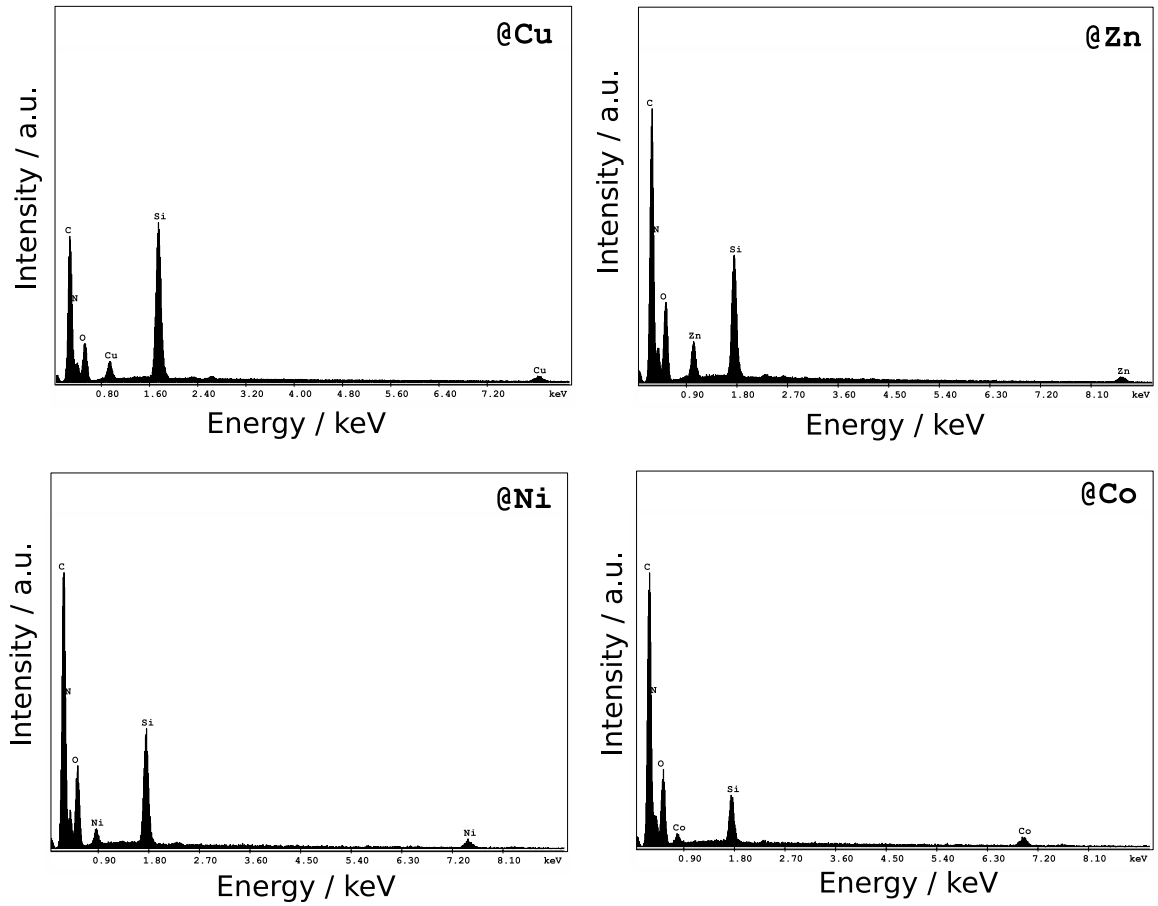

Figure S5. Metal-imidazole assessment by Raman and Infrared spectroscopy. A) Raman spectra of imGOx and MOEAs. The spectral region between 1530 and 1610 cm^{-1} is zoomed-in for details. . In absence of metal ions, i.e. imGOx sample, a characteristic Raman peak at ~1560 cm^{-1} is observed and assigned to the deprotonated Nτ-H form of imidazole. @Cu, @Zn, @Ni, and @Co MOEAs show a new band that is shifted to ~1584 – ~1589 cm^{-1} range (with one asterisk in the Figure). These new bands are characteristic of the presence of the imidazole-metal tautomer [Nτ-M; Nπ-M]. Moreover, a new band at ~1555 cm^{-1} (with two asterisks in the Figure), which may indicate the presence of metal-bridging imidazolate form (M-Im-M), is present in all MOEA samples.[1,2]
B) FTIR spectra of same samples. The spectral region showed in Figure 1C is highlighted within the box.

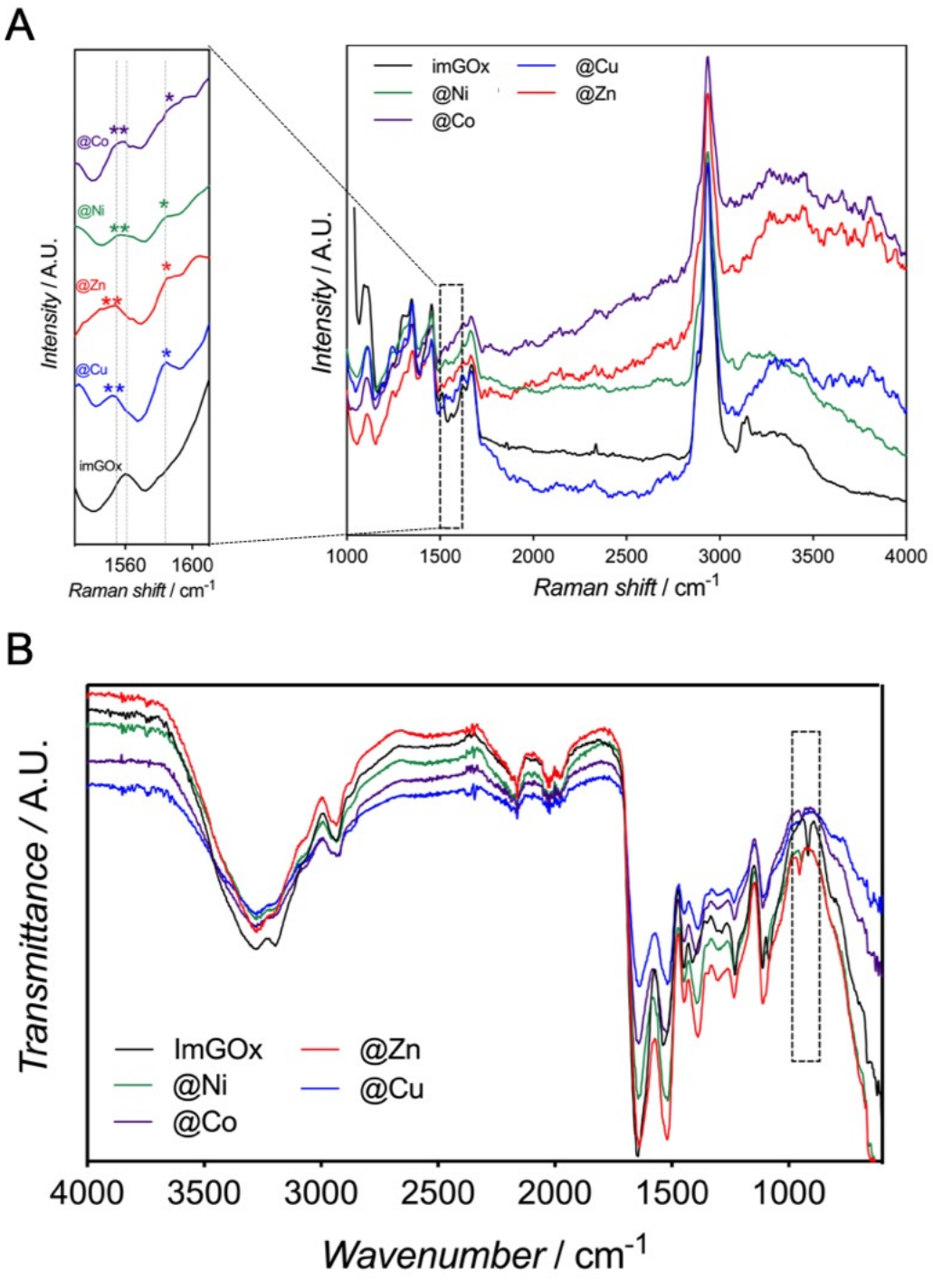

Figure S6. ATR-FTIR of GOx@Zn MOEA compared to GOx@Zn ZIF-8 composites in the 900-980 cm^{-1} spectral window. The peak at 956 cm^{-1}, which correspond to Zn-imidazole interaction, coincides in both hybrids. In this case, as the synthesis of @Zn MOEA was prolonged for 72h, the peak at 917 cm^{-1} (uncoordinated imidazole) has almost disappeared.

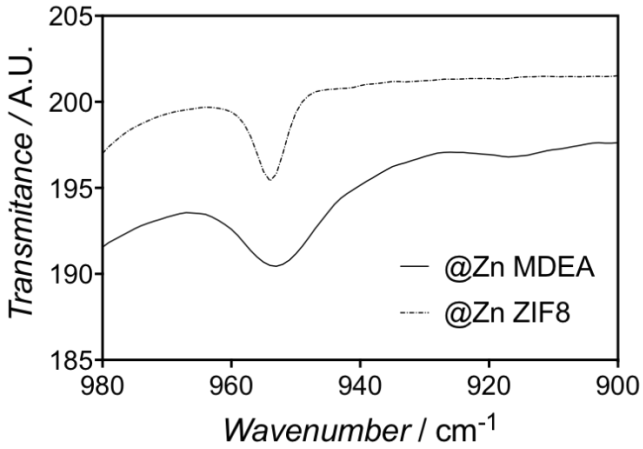

Figure S7. Statistical size distribution of @Cu, @Co, @Zn, and @Ni MOEA hybrids by Dynamic Light Scattering (DLS). Average sizes of ~1100, 550, 450, and 400 nm were measured for @Cu, @Zn, @Co, and @Ni MOEAs, respectively. A DLS-polydispersity value of 0.1 was obtained.

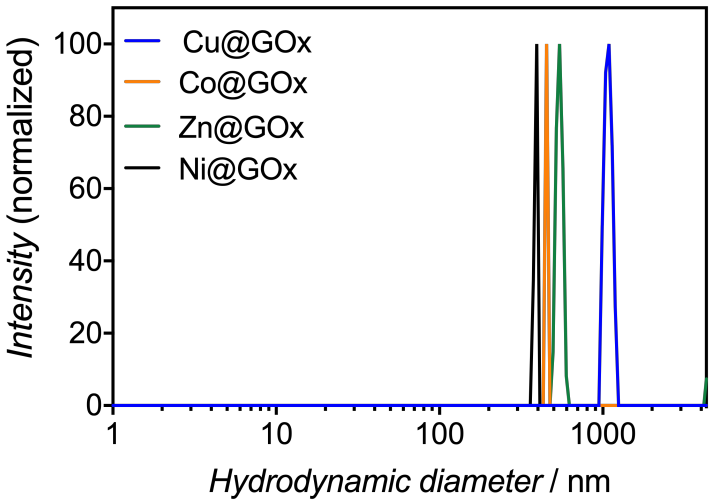

Figure S8. Detailed pictographs of GOx@Cu, GOx@Ni, GOx@Zn, and GOx@Co MOEA nanoparticles revealed by ESEM. (Scale bar: 600 nm).

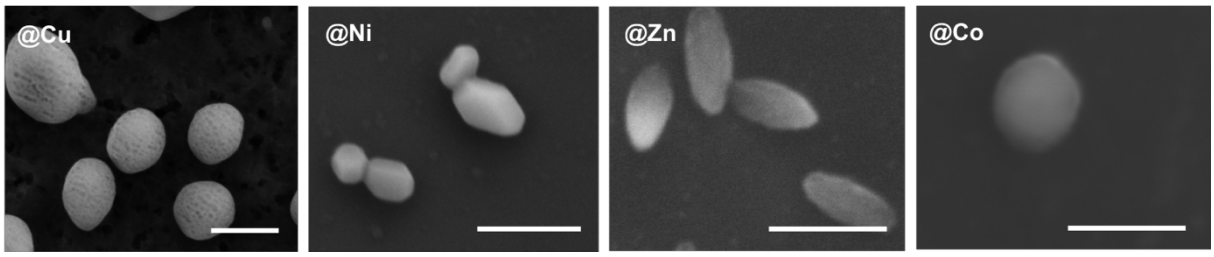

Figure S9. MOEAs synthesized at high protein concentration. A) ESEM pictograph of GOx@Cu aggregates synthesized with 0.5 mg ml^{-1} of GOx@imNG and 5 mM of $Cu(SO_4)_2$ in Tris buffer (30 mM, pH 7.0) (scale bar: 2 µm). B) MOEA hybrids synthesized with 2 mg ml^{-1} of GOx@imNG and 5 mM of respective metal salts dispersed in water. C) MOEA pellets (2 mg ml^{-1} of GOx@imNG and 0.5 mM of respective metal salts) could not be dispersed and are decanted on the bottom of the vial.

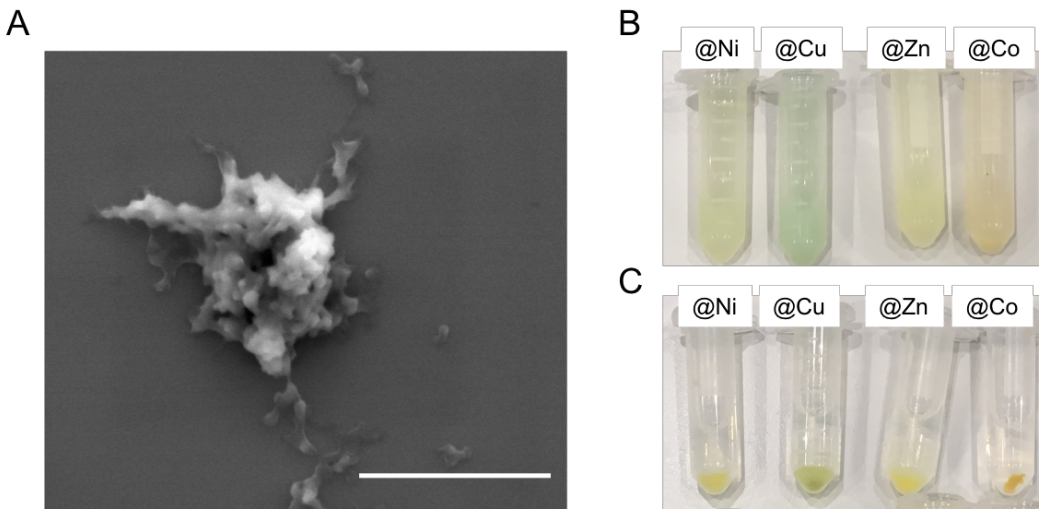

Figure S10. ATR-FTIR spectra comparison of @Cu MOEAs fabricated in Tris buffer (30 mM, pH 7.0), acetate buffer (30 mM, pH 5.0), and water. Zoomed region (960-900 cm-1) evidences a more effective coordination of imidazole molecules when Tris buffer is used (it shows a higher υ_{953}:υ_{917} ratio).

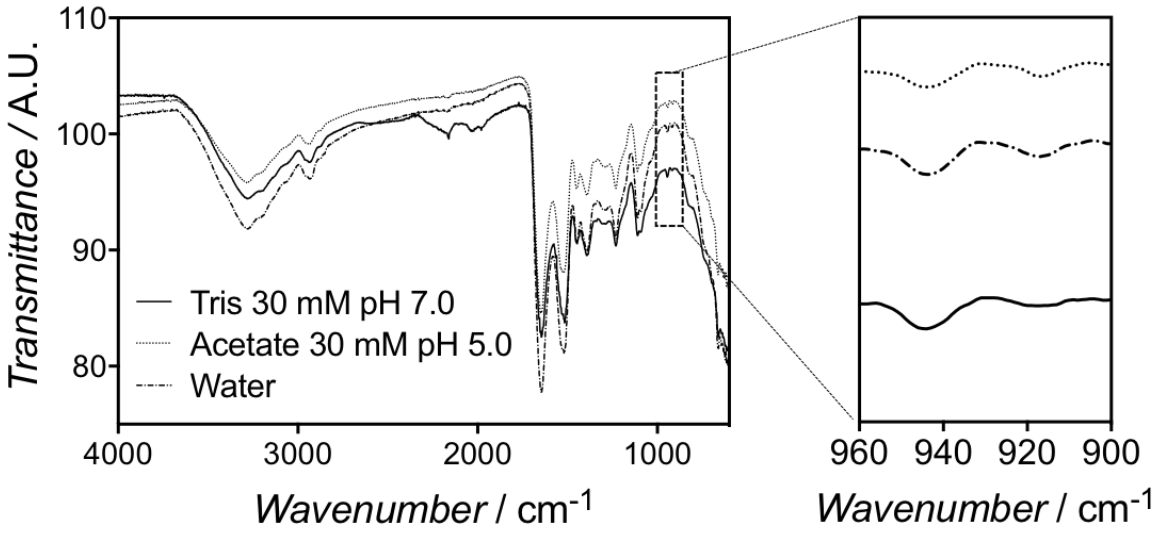

Figure S11. ATR-FTIR normalized spectra of GOx@Cu MOEAs fabricated in Tris buffer (@Cu) and phosphate buffer (@Cu-P).

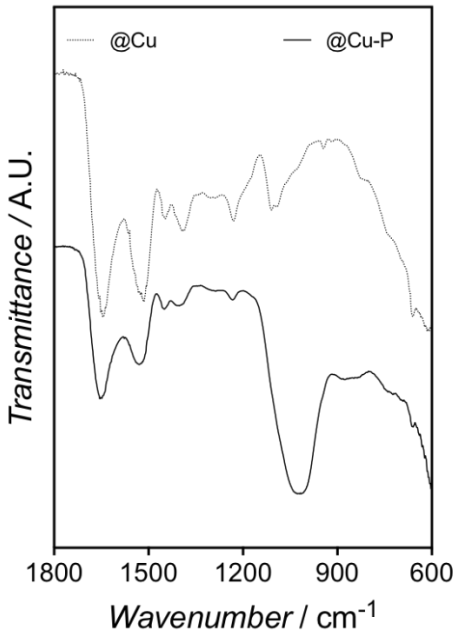

Figure S12. A) Magnified XPS spectra of the region corresponding to phosphorus measured from GOx MOEAs fabricated in Tris (GOx@Cu) and phosphate (GOx@Cu-P) buffer. B) Photographs showing the color of the solid precipitates obtained from GOx@Cu and GOx@Cu-P samples.

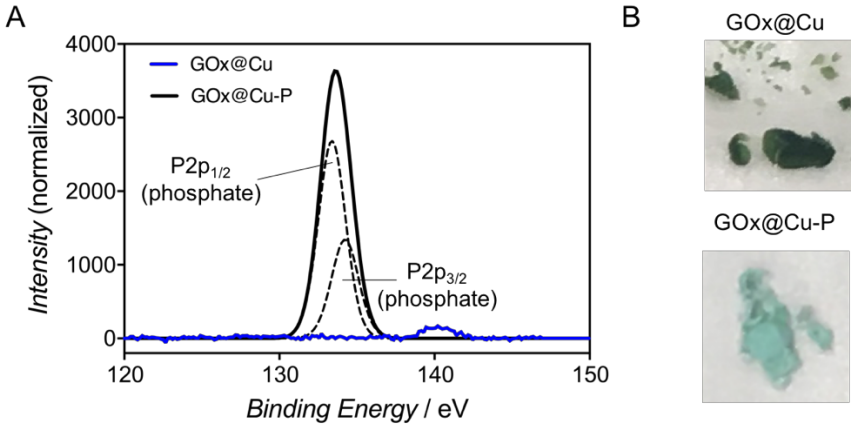

Figure S13. ESEM pictographs of GOx@ZIF-8#1 and GOx@ZIF-8#2 composites synthesized following published protocols.[3,4] An average particle size of 300 nm and 1.1 µm were measured by DLS for GOx@ZIF-8#1 and GOx@ZIF-8#2 samples, respectively.

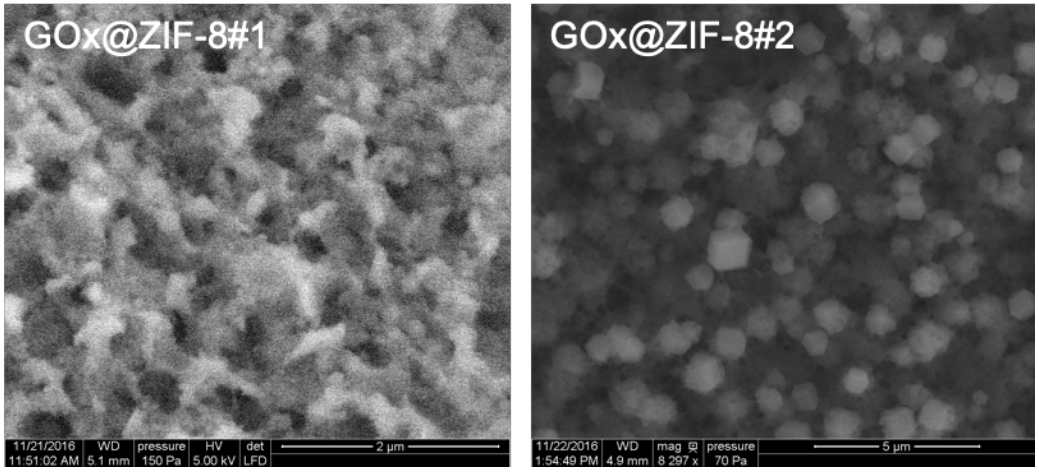

Figure S14. Glucose oxidation catalytic rates expressed as U per mg of solid measured for @Cu, @Ni, @Co, and @Zn assemblies fabricated in presence of phosphate buffer.

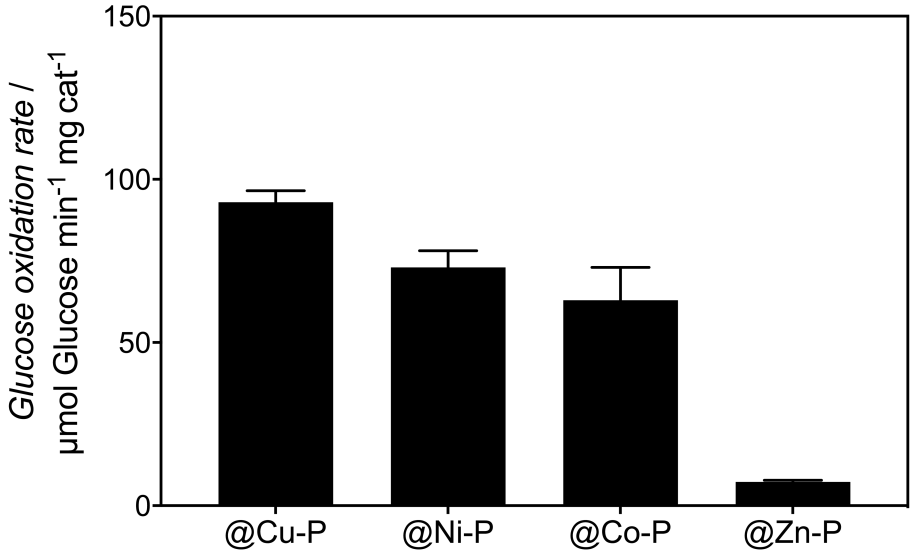

Figure S15. The loss of the tertiary structure of the protein is demonstrated by circular dichroism. Near-UV CD spectra (A) and traces of the CD signal at 270 nm (B) of GOx at a temperature gradient from 30 to 100°C.

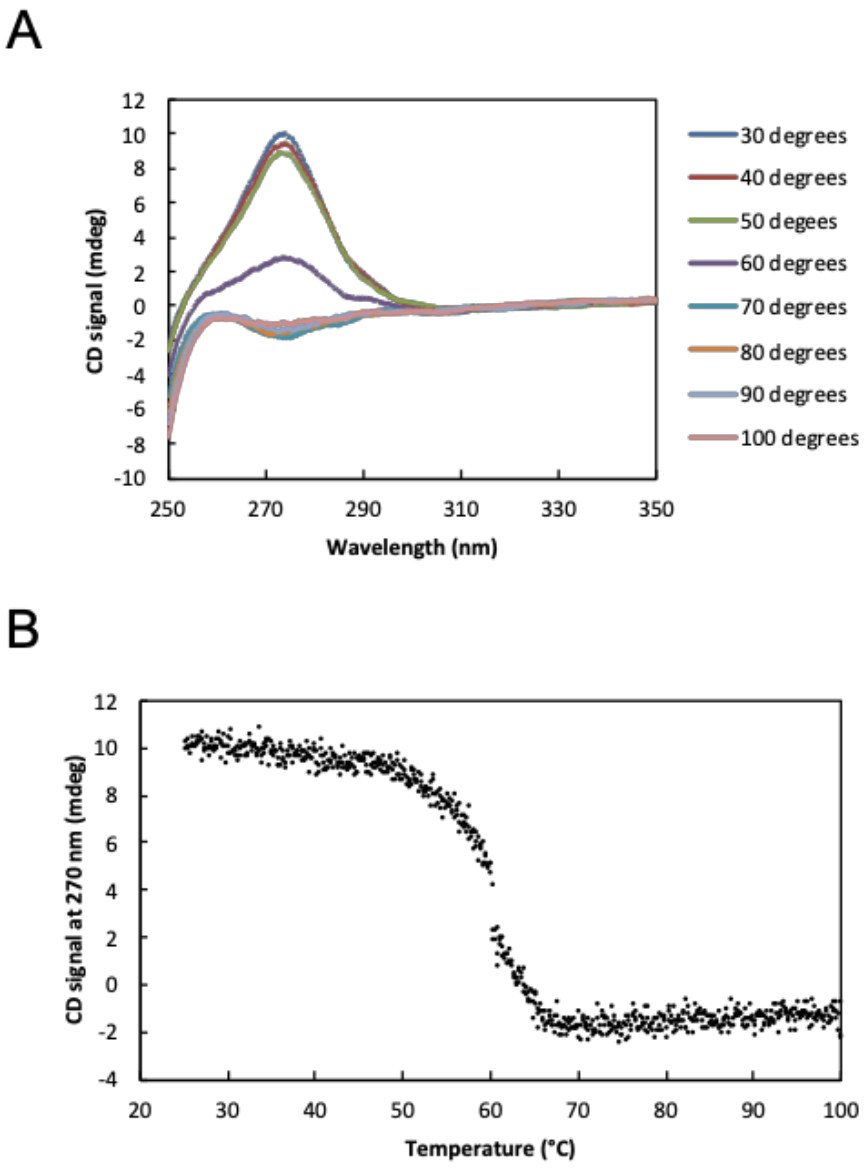

REFERENCES

(1) H. Takeuchi, “Raman structural markers of tryptophan and histidine side chains in proteins,” *Biopolym. - Biospectroscopy Sect.*, **2003**, *72*, 305–317.

(2) F. Jehle, P. Fratzl, and M. J. Harrington, “Metal-Tunable Self-Assembly of Hierarchical Structure in Mussel-Inspired Peptide Films,” *ACS Nano*, **2018**, *12*, 2160–2168.

(3) Lyu, F.; Zhang, Y.; Zare, R. N.; Ge, J.; Liu, Z. One-Pot Synthesis of Protein-Embedded Metal-Organic Frameworks with Enhanced Biological Activities. *Nano Lett.* **2014**, *14*, 5761–5765.

(4) Chulkaivalsucharit, P.; Wu, X.; Ge, J. Synthesis of Enzyme-Embedded Metal-Organic Framework Nanocrystals in Reverse Micelles. *RSC Adv.* **2015**, *5*, 101293–101296.